Bioactive Materials 6 (2021) 1353–1364

Contents lists available at ScienceDirect

Bioactive Materials

journal homepage: www.sciencedirect.com/journal/bioactive-materials

Surface decoration of development-inspired synthetic N-cadherin motif via Ac-BP promotes osseointegration of metal implants

Meiling Zhu [a,b,c], Kunyu Zhang [d], Lu Feng [a,b], Sien Lin [a,b,e], Qi Pan [a,b], Liming Bian [d,e,f,**], Gang Li [a,b,e,*]

[a] Department of Orthopaedics & Traumatology, Faculty of Medicine, The Chinese University of Hong Kong, Prince of Wales Hospital, Shatin, Hong Kong, SAR, PR China
[b] Stem Cells and Regenerative Medicine Laboratory, Li Ka Shing Institute of Health Sciences, The Chinese University of Hong Kong, Prince of Wales Hospital, Shatin, SAR, Hong Kong, PR China
[c] The Eighth Affiliated Hospital, Sun Yat-Sen University, Shenzhen, PR China
[d] Department of Biomedical Engineering, The Chinese University of Hong Kong, Hong Kong, SAR, PR China
[e] Shenzhen Research Institute, The Chinese University of Hong Kong, Shenzhen, PR China
[f] Centre of Novel Biomaterials, The Chinese University of Hong Kong, Hong Kong, SAR, PR China

ARTICLE INFO

Keywords:
N-cadherin mimetic peptide
Mesenchymal condensation
Osseointegration
Wnt/β-catenin signaling
Titanium dioxide (TiO_2)

ABSTRACT

Research works on the synergistic effect of surface modified bioactive molecules and bone metal implants have been highlighted. N-cadherin is regarded as a key factor in directing cell–cell interactions during the mesenchymal condensation preceding the osteogenesis in the musculoskeletal system. In this study, the N-cadherin mimetic peptide (Cad) was biofunctionalized on the titanium metal surface via the acryloyl bisphosphonate (Ac-BP). To learn the synergistic effect of N-cadherin mimetic peptide, when tethered with titanium substrates, on promoting osteogenic differentiation of the seeded human mesenchymal stem cells (hMSCs) and the osseointegration at the bone-implant interfaces. Results show that the conjugation of N-cadherin mimetic peptide with Ac-BP promoted the osteogenic gene markers expression in the hMSCs. The biofunctionalized biomaterial surfaces promote the expression of the Wnt/β-catenin downstream axis in the attached hMSCs, and then enhance the in-situ bone formation and osseointegration at the bone-implant interfaces. We conclude that this N-cadherin mimetic peptide tethered on Ti surface promote osteogenic differentiation of hMSCs and osseointegration of biomaterial implants *in vitro* and *in vivo*. These findings demonstrate the importance of the development-inspired surface bioactivation of metal implants and shed light on the possible cellular mechanisms of the enhanced osseointegration.

1. Introduction

N-cadherin is a transmembrane protein considered to be the key factor in directing cell-cell interactions during the mesenchymal condensation [1,2]. Cell-cell interactions and the formation of tight mesenchymal aggregates during the mesenchymal condensation are the earliest morphogenetic events preceding the development of several musculoskeletal tissues such as cartilage and bone [3,4]. We have previously shown that the conjugation of a N-cadherin mimetic peptide in hydrogel scaffold promotes the osteogenesis of stem cells and bone regeneration [3]. Study by others also demonstrates the HAVDI/N-cadherin interactions can alter stem cell perception of the stiffening extracellular microenvironment [5]. Therefore, in this study, the effects of this N-cadherin mimetic peptide to promote MSCs osteogenesis and implant osseointegration, when tethered with metal substrate, are further examined [6].

There has been extensive research on the bioactive molecules including biomimetic peptides (e.g., Arg-Gly-Asp, RGD) for increasing cell affinity of metal substrate [7,8]. Because of the biocompatible and corrosion-resistant properties of the surface titanium oxide layer (TiO_2) [7,9,10], titanium is one of the most biocompatible metallic biomaterials with a long history of use in orthopedic and dental implants.

* Corresponding author. Room 74038, 5 F, Lui Chee Woo Institute Clinical Science Building, Prince of Wales Hospital, Shatin, NT, Hong Kong, SAR, PR China.
** Corresponding author. Room 1106, William M.W. Mong Engineering Building, Department of Biomedical Engineering, The Chinese University of Hong Kong, Shatin, Hong Kong, PR China.
E-mail addresses: lbian@cuhk.edu.hk (L. Bian), gangli@cuhk.edu.hk (G. Li).

https://doi.org/10.1016/j.bioactmat.2020.11.002
Received 8 July 2020; Received in revised form 25 October 2020; Accepted 1 November 2020

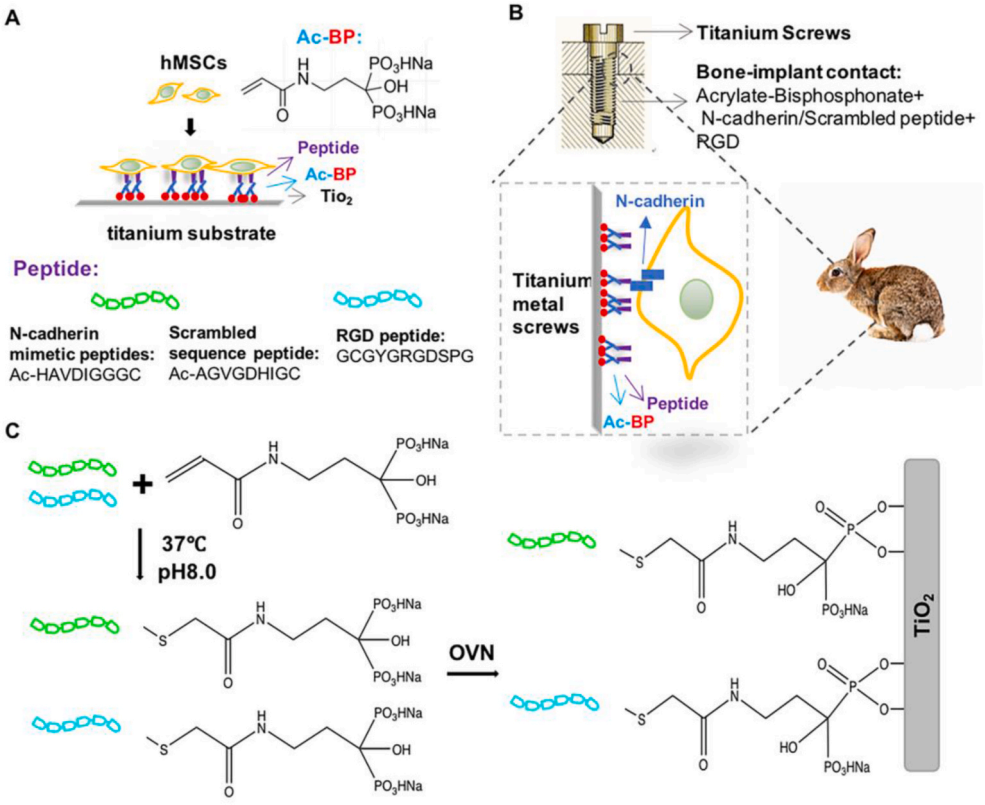

Fig. 1. (A) Diagram illustrating biomimetic peptide/acryloyl-bisphosphonate (Ac-BP) conjugation and hMSCs seeding on 2D titanium substrates, (B) osseointegration in the site of the implantation with the biomimetic peptide/Ac-BP conjugated titanium screws in rabbit tibiae/femurs (*in vivo*). (C) And the reaction of biomimetic peptide conjugation to TiO_2 substrates with Ac-BP.

Despite numerous prior studies [11,12], there is still acute demand to identify novel bioactive molecules which can promote the osseointegration when coupled with titanium and other metal implants [13], which may also solve the clinical issues of the Ti implants due to the non-specific cell adhesion and insufficient osseointegration [8,14].

Meanwhile, efficient conjugation of bioactive molecules on metal substrates is a challenging task [10,15]. A wide variety of methods have been developed to conjugate bioactive peptides/proteins [6,16,17] and other bioactive molecules to the surface of titanium by employing physical interactions or chemical conjugations [18–21] of various functional groups. Bisphosphonates (BP), are a class of drugs that have been reported to suppress osteoclastic activities for treating osteoporosis [22], therefore, the application of Ac-BP in our study are with high bio-safety. BP also shows excellent binding affinity to the mineralized tissues such as bone, metal surfaces, and other inorganic nano-structures [22–25]. One previous study demonstrated the attachment of bioactive molecules to metal substrate via the conjugated BP group [26]. Furthermore, in this study we capitalized the metal-binding capability of BP to conjugate biomimetic peptide to implant metal surface.

This study aims to learn about the synergistic effect of N-cadherin mimetic peptide and Ti to improve the osseointegration of implants through surface immobilization methods. The N-cadherin mimetic peptide was biofunctionalized on the titanium metal surface via the acryloyl bisphosphonate (Ac-BP) to learn about the change of cell adhesion, osteogenesis *in vitro* and also the osseointegration of implants *in vivo*. We hypothesize that the N-cadherin mimetic peptide biofunctionalized substrates and surface of implant with BP molecule would promote the osteogenic differentiation of seeded human bone mesenchymal stem cells (hMSCs) and enhance the in situ osseointegration. The Wnt/β-catenin pathway is one of the important molecular cascades that regulate cell fates throughout lifespan [27,28]. Herein, we also investigate the possible signaling pathways, of either the Wnt/β-catenin [29–32] or PI3K axis [33,34], during osteogenesis process of the seeded MSCs on the biofunctionalized titanium surface.

2. Materials and methods

2.1. Macromere synthesis and coating preparation

2.1.1. Biomimetic peptide

N-cadherin (Ac-HAVDIGGGC) (Peptide 2.0) mimetic or scrambled sequence (Ac-AGVGDHIGC) (Peptide 2.0) peptide and RGD (GCGYGRGDSPG) (GenScript) peptide (GenScript) with a cysteine residue at the C-terminal.

2.1.2. Synthesis of acryloyl bisphosphonate (Ac-BP)

N-acryloxysuccinimide and pamidronate disodium salt were dissolved in NaOH solution (pH = 8.0) together and stirred for reaction. After 24 h reaction at room temperature, the crude product was precipitated from water upon the addition of absolute ethanol. The precipitate was collected by centrifugation and washed with ethanol for several times [22,35].

2.1.3. Preparation of 2D coating substrate and the implantation screws

The mimetic peptides were conjugated with the Acryloyl-bisphosphonate (Ac-BP) molecule by the reaction between the thiol group of the C-terminal and the double bond of the molecule of Ac-BP in alkaline phosphate buffer (0.2 M Na_2HPO_4–NaH_2PO_4, pH 8.0) at 37 °C overnight with the supplementary of TCEP (tris (2-carboxyethyl) phosphine) (10 mM) as reducing agent. The obtained reaction solution was used to coat on the surface of the titanium plate (TiO_2), and the peptide-bisphosphonate compounds can be reacted on the metal surface. For the coating of the implanted screws, TiO_2 screws should be soaked in the reaction solution overnight before the surgery of the implantation on the

sites of the rabbit knee joints (Fig. 1C).

2.2. Cell culture and seeding on 2D substrate

Human MSCs (Lonza) were expanded to passage 3 in growth media containing α-MEM with 10% FBS (Fetal Bovine Serum), 1% PSN (Penicillin-Streptomycin-Neomycin). Human MSCs (5000 cells/cm^2) were cultured on the 2D peptides/Ac-bisphosphates conjugated substrates (6 mm * 7 mm, 0.5 mm thickness), which were conjugated with Ac-bisphosphate, the N-cadherin mimetic peptide and RGD peptide (Cad + RGD), scrambled sequence peptide and RGD peptide (Scram + RGD), or with RGD peptide (RGD) alone. The molar ratio between the acryloyl groups and the peptide thiols is 10 (acryloyl): 11 (peptide thiol). The substrates were then cultured in osteogenic media (α-MEM, 16.67% FBS, 1% glutamine, 10 mM β-glycerophosphate disodium, 50 μg/ml ascorbate, 100 nM dexamethasone), which was changed three times per week, and evaluated at selected time points.

2.3. Staining of the biological markers on 2D substrates

Human MSCs seeded on the 2D biomimetic peptide/Ac-BP functionalized titanium substrates were fixed in 4% paraform for 10 min, rinsed in phosphate-buffered saline (PBS) for at least three times, and permeabilized with 0.25% TritonX-100 in PBS for 30 min at room temperature. For immunofluorescence staining of RUNX2 marker, samples were blocked with 0.5% bovine serum albumin (BSA) in PBS for 30 min at 37 °C after permeabilization. Samples were incubated with primary antibodies (1: 100 dilution) in 0.5% BSA at 4 °C overnight, and subsequently with secondary antibodies (1: 200 dilution) in blocking solution for 2 h at room temperature. To estimate the RUNX2 expression, Image J was used to measure the ratio between the nuclear and cytoplasmic fluorescence intensity of the hMSCs stained with a RUNX2 antibody (mouse monoclonal anti-RUNX2, Santa Cruz), and the staining of DAPI for nuclei as a counterstain [3].

2.4. Atomic force microscope analysis

AFM contact mode were applied at a swiping force of increasing magnitude on the surface of the titanium substrates by increasing the deflection setpoint voltage (V) from 1.000 V to 10.000 V. We observed that the TiO_2 substrates are almost cleared by the AFM tip when setpoint voltage is increased to 10.000 V in the absence of magnetic field (the test area of AFM analysis is 10 μm*10 μm).

2.5. X-ray photoelectron spectroscopy

XPS spectra were acquired using EscaLab 250Xi, AI X-ray source (hv = 1486.6 eV, tube voltage = 15 kV, tube current = 12 mA, 180 W). The fitting procedure was carried out by using CasaXPS software.

2.6. RNA isolation and real-time PCR

Total RNA was isolated by using Trizol (Thermo Fisher Scientific) for seeded hMSCs, then reverse transcribed using PrimeScrip RT reagent Kit (Takara Bio, Tokyo, Japan). Real-time PCR was performed with SYBR Green PCR Master Mix (Applied Biosystems, Foster City, CA, USA). Glyceraldehyde-3-Phosphate Dehydrogenase (GAPDH) was used as the internal control for mRNA expression, and gene expression changes were quantified by using the ΔΔCt method. Real-time PCR was performed in duplicate. Primer sequences for real-time PCR are list in Table S1.

2.7. Western blot analysis

Total protein was isolated from the cultivated cells by using RIPA Lysis Buffer (Thermo Fisher Scientific) with the addition of 1% protease inhibitor (Roche). For the extraction of cytoplasm or nuclear protein, cytoplasm or nuclear extraction buffer was used [3]. Equal amounts of protein were loaded for electrophoresis. Soluble protein was separated by SDS-PAGE followed by a semidry transfer to PVDF (Polyvinylidene fluoride membrane). Membranes were blocked for 1 h with 5% nonfat milk, then incubated with primary antibody, namely anti-β-catenin (1: 10000), anti-GAPDH (1: 10000) at 4 °C overnight. After being washed in Tris-buffered saline containing Tween, membrane was incubated with horseradish peroxidase-conjugated secondary antibodies (anti-mouse, Santa Cruz Biotechnology) for 1 h at room temperature. The blot was then developed with Amersham ECL Western Blotting Detection Reagent (GE Healthcare, Waukesha, WI, USA) according to manufacturer instructions.

2.8. Luciferase assay

Dual-luciferase assay was performed to evaluate the luciferase activity of the reporter constructs according to the instructions of dual-luciferase assay reagents (Promega, USA) with some modifications [3]. In brief, hMSCs were cultivated on cell culture plate, and the cells were allowed to grow until 80% confluency. Cells were then transfected with TOPFlash or pmiR-GLO luciferase reporter plasmids together with β-catenin expression vectors or miRNA mimics. The pRSV-β-galactoside (ONPG) vector was co-transfected into hMSCs as an internal control for normalization. The plate was placed into a PerkinElmer VictorTM X2 2030 multilabel reader (Waltham, USA) to measure the firefly luciferase activity, as well as the β-galactosidase activity. The ratio of firefly luciferase to β-galactosidase activity in each sample was revealed as a measurement of the normalized luciferase activity. All experiments were performed in triplicate.

2.9. Animal study

2.9.1. Surgical protocol for in vivo implantation and experimental design

For the implantation, six skeletally matured New Zealand white rabbits (male, body weight 2.0–2.5 kg) were used in this study. All the animal work followed the guidance of the European Commission Directive 86/609/EEC for animal experiments with proper animal experimental ethical approval. Under general anesthesia and sterile conditions, a small incision was made at the medical aspect of the knee joint at both legs to expose the medical proximal tibial plateau and medial distal femoral condyle. A 3.5 mm diameter hole (screws of 12 mm in length) was pre-drilled and then testing screw was carefully screwed into position, and the skin was sutured. Each rabbit had 4 various screws implanted at both femurs and tibiae in a randomly mixed fashion, total 6 screws from each group were implanted. All rabbits were sacrificed at 8 weeks after the implantation and the femurs and tibiae were harvested.

2.9.2. Torque removal force measurement

Screws (n = 4 per group) were used to determine the torque removal force using a manual torque meter (clutch release torque screw driver) according to the manufacturer's instruction (Model: N6-50LTDK, Kanon, Nakamur Company, Tokyo, Japan). The torque force used to unscrew the implanted screws were recorded and compared.

2.9.3. Ex vivo micro-CT and histomorphometric analysis

Samples with the implanted screws (n = 3 per group) were scanned and analyzed by micro-CT 40 (ScancoMedical, Sweden). A region of the proximal tibia/femurs with 20 mm in length covering the drill-hole site at a voltage of 70 keV with a current of 114 μA. After automatic reconstruction, 2D slices with 19 μm isotropic resolution were generated and used to select the region of interest (ROI), the same as which described in DXA (Dual-energy x-ray absorptiometry) analysis for 3D reconstruction. After choosing a threshold (sigma = 1.2, support = 2 and threshold = 190), the bone volume fraction (BV/TV) (Fig. S6) will be

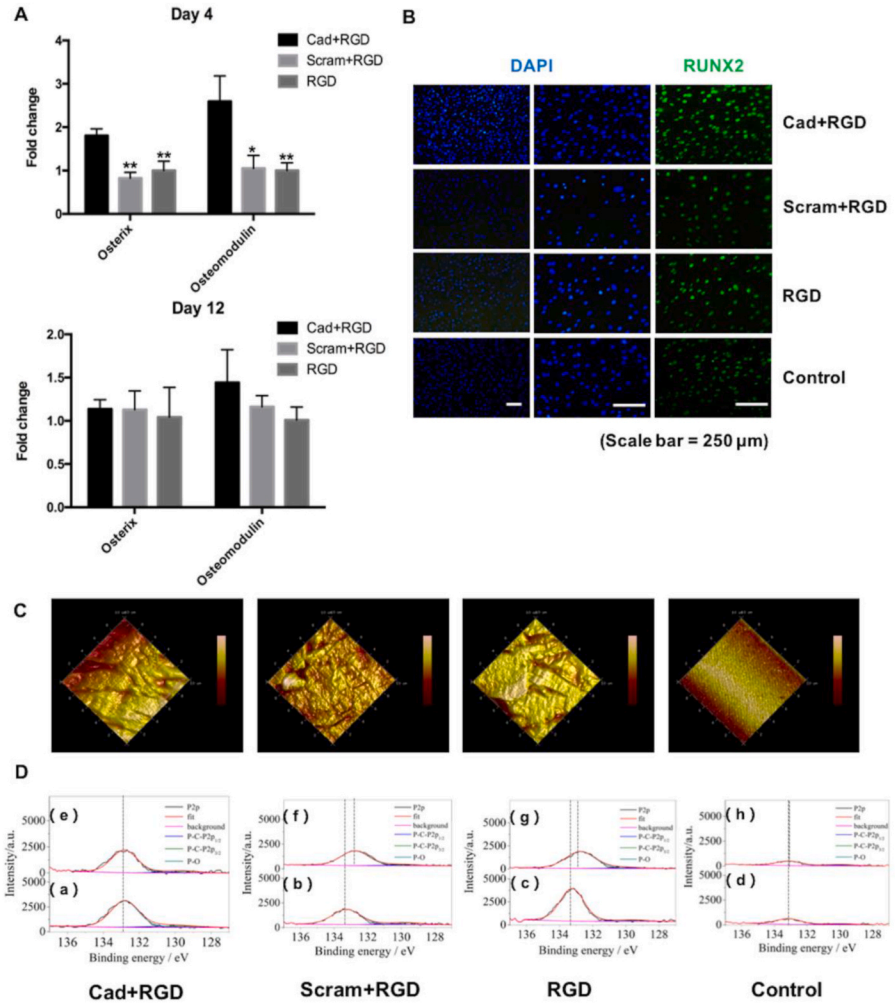

Fig. 2. (A) Gene expression of osteogenic markers (Osterix and Osteomodulin) in the hMSCs seeded on the biomimetic peptide/Ac-BP conjugated TiO_2 surface after osteogenic differentiation for 4 days and 12 days. (*p value < 0.05, **p value < 0.01 vs. Cad + RGD, n = 4). (B) RUNX2 immunostaining of the hMSCs seeded on 2D titanium substrates (Control), and the substrates conjugated with Ac-BP and N-cadherin/RGD mimetic peptide (Cad + RGD), Scrambled sequence N-cadherin/RGD mimetic peptide (Scram + RGD), or RGD mimetic peptide (RGD) after 4 days of osteogenic culture. (Scale bar = 250 μm) (C) The atomic force microscope (AFM) images of group Cad + RGD, Scram + RGD, RGD and control. The untreated titanium substrates were measured as control (The test area of AFM analysis is 10 μm*10 μm as shown in figure). (D) X-ray photoelectron spectroscopy (XPS) spectra of corresponding groups (a–d) to the AFM scanning result, showing P–O peaks after the reaction with biomimetic peptide/acryloyl-bisphosphonate and washed with distilled water. While images (e–h) also show the grouped peaks measured 12 days after the surface coating reaction, which demonstrated the successful reaction of Ac-BP and biomimetic peptide on the titanium surface by forming titanium-oxygen-phosphorus group (Ti–P–O), and the coating would last after 12 days cultivation (n = 3).

calculated using built-in software.

2.9.4. Histological evaluations

Histological examination isolated tibiae/femurs were fixed in 10% neutral-buffered formalin, transferred to 70% ethanol, and decalcified in 10% EDTA. After tissue processing, the specimens were embedded in paraffin. Sections (5 μm) were cut coronally along the tibial shaft axis and collected on glass slides, deparaffinized, and subjected to hematoxylin and eosin (H&E) staining using standard protocols. After mounting with coverslips, the specimens were viewed and analyzed under a light microscope (Leica DMRB DAS; Leica, Heerbrugg, Switzerland).

The sequential fluorescence labeling was used to evaluate new-bone formation rate or bone remodeling during fracture healing, as previously reported [36–38]. Calcein green (5 mg/kg, Sigma-Aldrich, USA) was subcutaneously injected into rat femora 1 week (at week 6) before xylenol orange (90 mg/kg, Sigma-Aldrich, USA) was injected in the same way. One more week afterward (at week 8), rabbits were sacrificed, and isolated tibiae/femurs (n = 2 per group) were collected and embedded in MMA (methyl methacrylate) without decalcification and sectioned into thick sections (200 μm). The tissue sections were further ground and polished to 100 μm for the evaluation of new-bone formation rate under a fluorescence microscope (Leica Q500MC, Leica, Germany). To calculate the temporal change of new bone formation, 5 mm proximal and 5 mm distal to the fracture line was chosen as the ROI for quantification of new bone formation. The ratio of area labeled with xylenol orange to area labeled with calcein green was determined using ImageJ [3].

2.10. Quantitative assay of the biological markers on 2D substrates

To estimate the RUNX2 and β-catenin expression, Image J was used to measure the ratio between the nuclear and cytoplasmic fluorescence intensity of the hMSCs stained with a RUNX2/β-catenin antibody (mouse monoclonal anti-RUNX2, Santa Cruz), and these followed by the staining of DAPI as a counterstain [3]. The rhodamine-phalloidin was used to stain F-actin and stabilize actin filaments of hMSCs, showing the cytoskeleton structure of cells on the substrate.

2.11. Statistical analysis

All data were presented as mean ± standard deviation. Statistical analysis was performed by using two-way ANOVA and Tukey's HSD post hoc testing to allow comparison between groups with experimental group as the independent factor (sample sizes are shown in the figure captions).

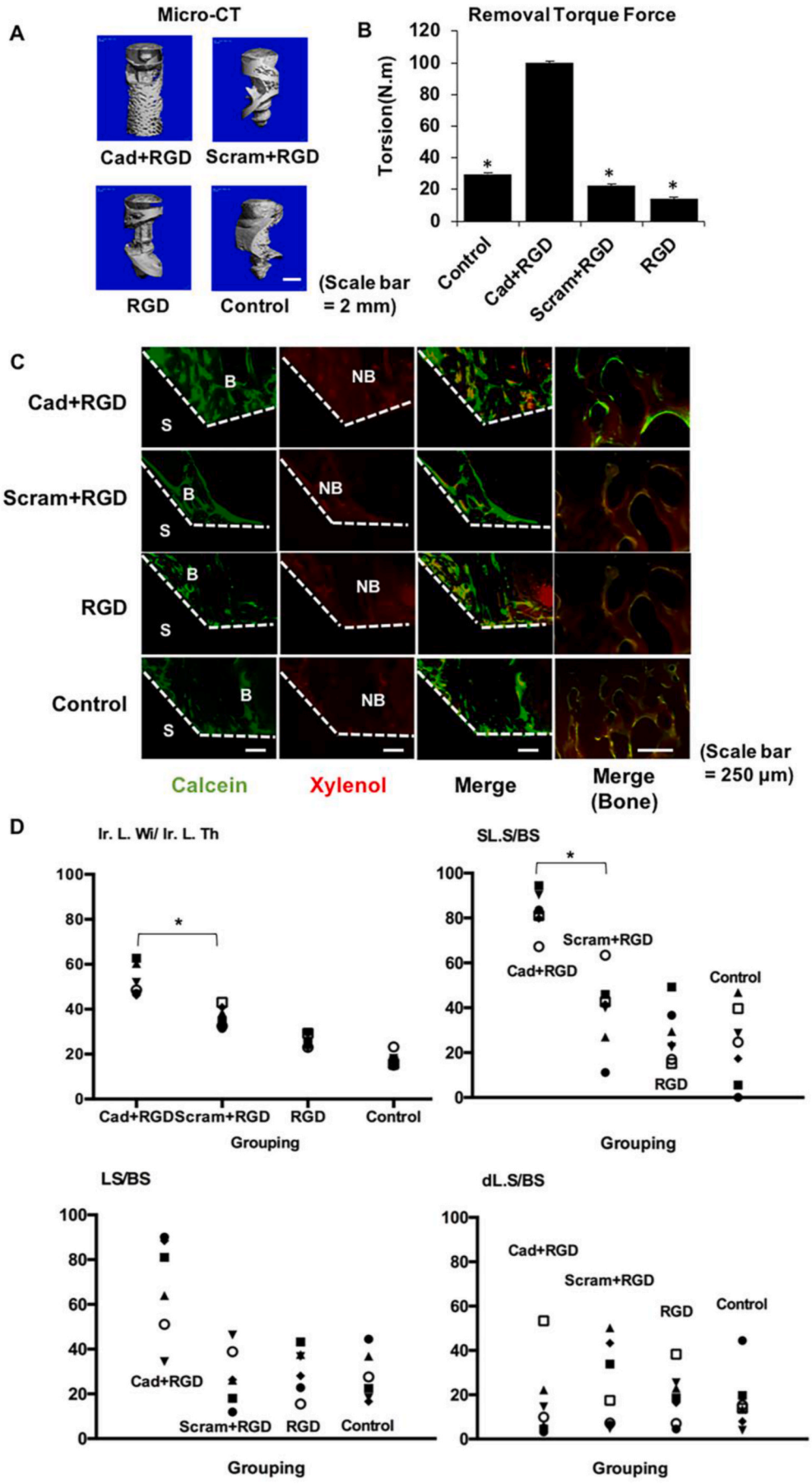

Fig. 3. (A) Micro CT reconstruction images (Scale bar = 2 mm), (B) removal torque force for screws and conjugated implants tested by the manual torque meter (*P value < 0.05 vs. Cad + RGD, n = 3), (C) bone-remodeling assessment by calcein/xylenol double-labeling (n = 7, one image from each of four rabbits per group) in rabbit tibiae/femurs 8 weeks after implantation with biomimetic peptide/Ac-BP conjugated screws (dotted line: interface of the implantation and the joint, B: native bone, NB: newly formed bone, S: implanted screw, Scale bar = 250 μm). (D) Effects of conjugation of biomimetic peptide on the titanium substrates as proximal tibiae/femurs metaphysis cancellous bone parameter, which shows the interface of N-cadherin mimetic peptide conjugated implants (Cad + RGD) accelerate the bone deposition (SL.S: single-labeled surface; dL.S: double-labeled surface; LS: labeled surface; BS: bone surface; L. Th: label thickness; L.Wi: label width; Ir. L. Wi/Ir. L. TH: mineral apposition rate) (*p value < 0.05, vs. Cad + RGD, n = 7).

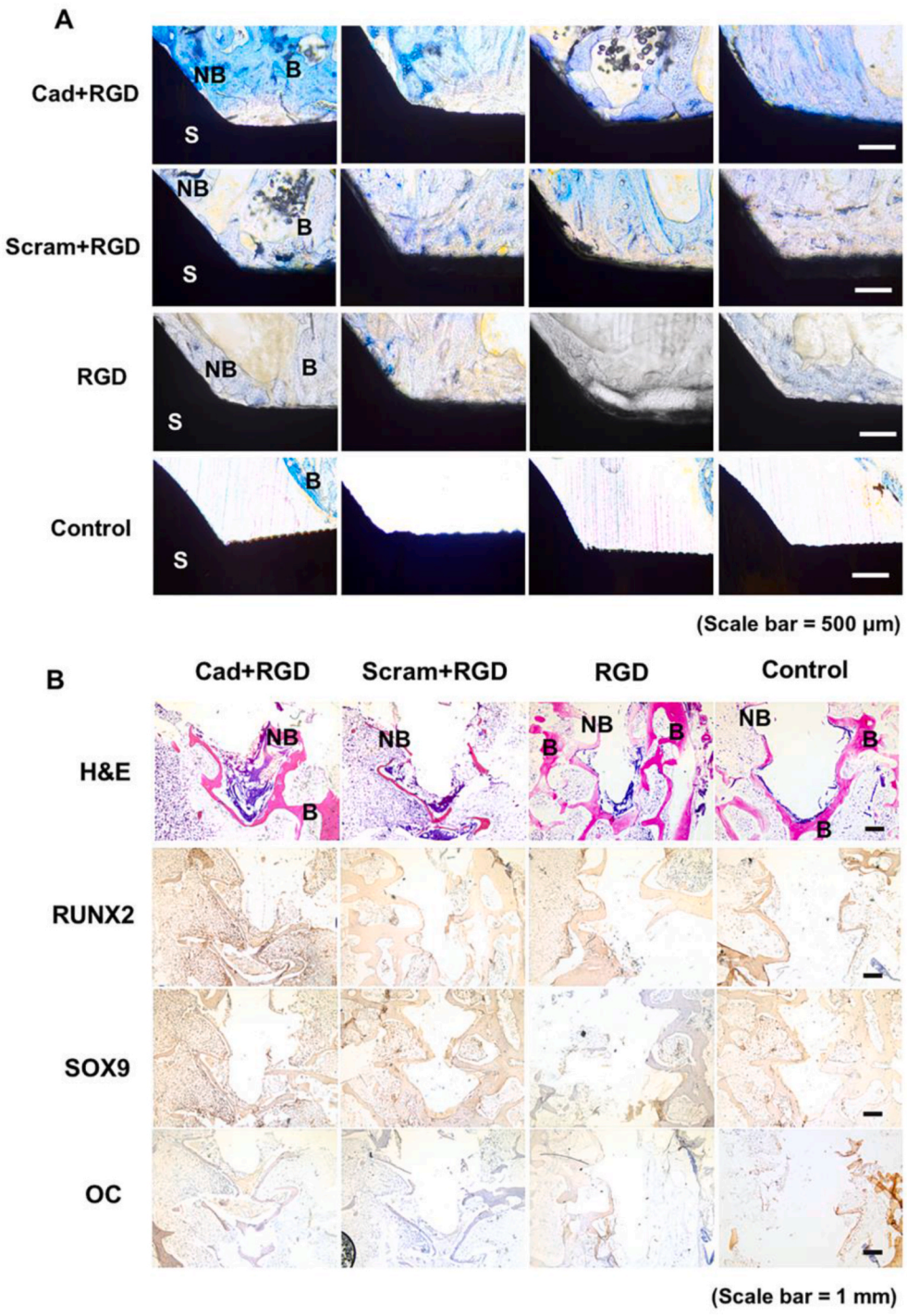

Fig. 4. Histological sections of screw implants and screws conjugated with biomimetic peptide/Ac-BP in the site of rabbit tibiae/femurs 8 weeks after implantation (A) MMA sections prepared by methyl blue staining (B: native bone, NB: newly formed bone, S: implanted screw, Scale bar = 500 μm). (B) Hematoxylin/eosin and Immunohistochemistry (RUNX2, SOX9 and Osteocalcin) staining of the paraffin sections of the tibiae/femurs after the remove of the implanted screws (B: native bone, NB: newly formed bone, Scale bar = 1 mm). The results show more bony tissue are observed in the samples of the N-cadherin mimetic peptide conjugated group (Cad + RGD) when compared to the control groups (Scram + RGD, RGD and control). The Immunohistochemistry images show more intense staining of the RUNX2, SOX9 and Osteocalcin in the N-cadherin mimetic peptide conjugated group, and this demonstrate that the osseointegration is significantly enhanced in the group conjugated with biomimetic peptide and Ac-BP. (For interpretation of the references to colour in this figure legend, the reader is referred to the Web version of this article.)

3. Result

3.1. The conjugation of mimetic peptide via acryloyl bisphosphonate (Ac-BP) on 2D titanium substrate enhanced the osteogenesis of the seeded hMSCs

Human MSCs were seeded on the 2D titanium substrates that were conjugated with the N-cadherin mimetic peptide (or the scrambled-sequence N-cadherin peptide with RGD peptide) via acryloyl bisphosphonate (Ac-BP), with cells seeded on the untreated titanium surface as the control group (Fig. 1A). The immunofluorescence staining revealed more intense RUNX2 staining in the Cad + RGD group compared to all the control groups (Scram + RGD, RGD, and untreated control) (Fig. 2B) after four days of osteogenesis *in vitro* culture. Compared to the control groups, the titanium substrates coated with N-cadherin mimetic peptide/Ac-BP significantly upregulated the mRNA expression of osteogenic markers including Osterix (118.5% higher vs. Scram + RGD, 80.3% higher vs. RGD) and Osteomodulin (146.7% higher vs. Scram + RGD, 159.4% higher vs. RGD) of the seeded hMSCs after four days of osteogenic differentiation (Fig. 2A). Nevertheless, the mRNA expression level of hMSCs showed no significant difference among different groups after 12 days under the osteogenic induction culture condition (Fig. 2A).

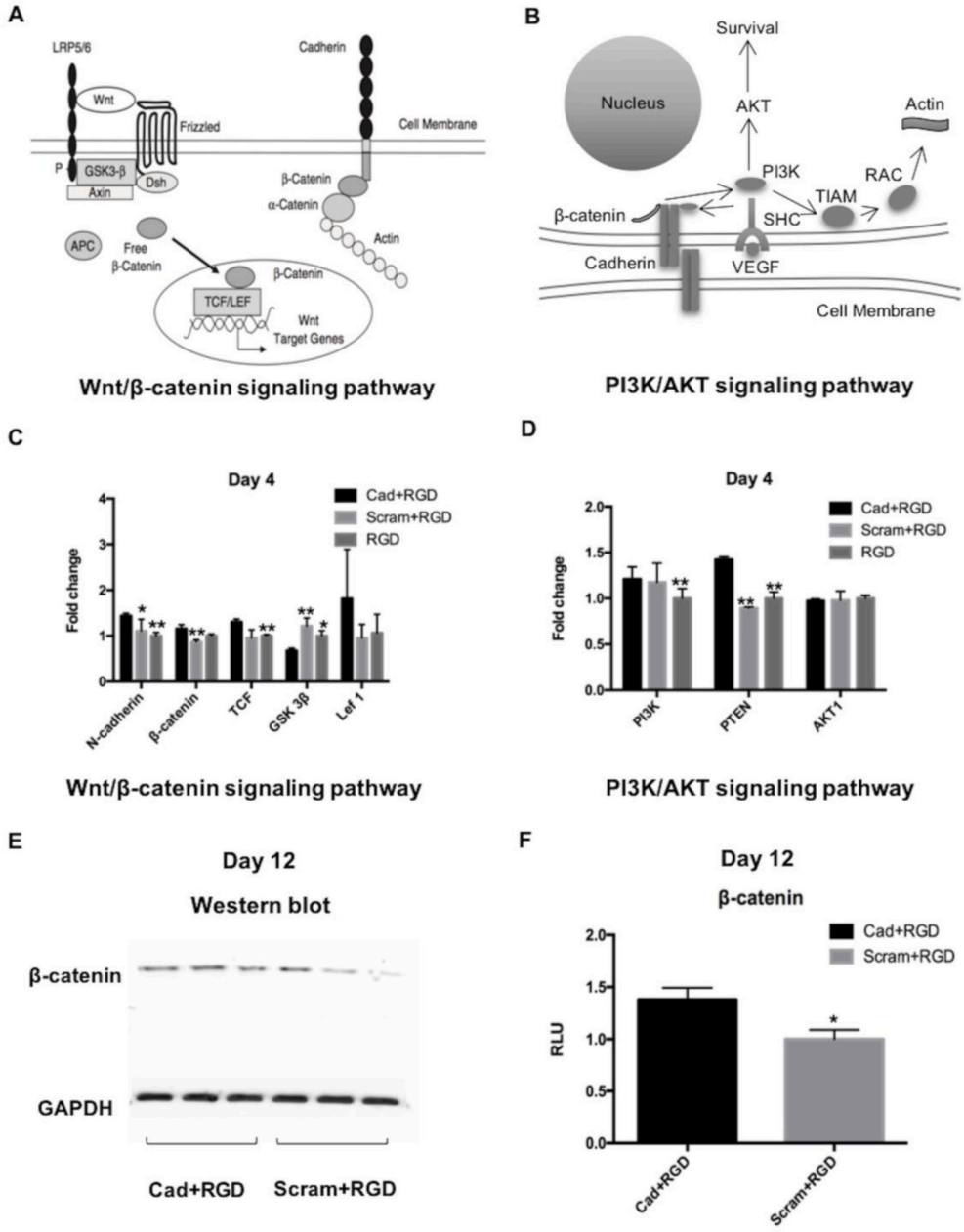

Fig. 5. Schematic diagrams showing the possible mechanisms of (A) Wnt/β-catenin and (B) PI3K/AKT axis in controlling osteogenesis. The mRNA expression level of (C) Wnt/β-catenin and (D) PI3K/AKT signaling pathway-related marker genes were examined by qRT-PCR assays (*p value < 0.05, **p value < 0.01 vs. Cad + RGD of day 4, n $= 4$). (E) Western blot of β-catenin showed that β-catenin was increased in the Cad + RGD group. (F) β-catenin activities were significantly increased in the Cad + RGD group by luciferase reporter assay (*p value < 0.05, n $= 3$).

3.2. The functionalization of bisphosphonates and biomimetic peptide on the surface of titanium last 12 days during in vitro cultivation

We did the AFM and XPS analysis to characterize the surface feature and chemical component of titanium substrates after the functionalization with biomimetic peptide and Ac-BP molecules, and also gain insight into the degradation of the functionalized layer. (A) The AFM data shows that the surface of substrates changed after the functionalization reaction, more rough features are observed after the surface coating reaction, when compared to the bold Ti substrates. (B) The P 2p peak of all the samples consists of three main components, namely P–O, P 2p1/2 and P 2p3/2 arising from the spin-orbit splitting in the p-type orbitals. The main peak of P–O should be attributed to the reaction between the Ac-BP to the titanium substrate. Moreover, the Michael-addition reaction between the thiol group of biomimetic peptide and acrylic acid group has been reported in our previous study [3]. According to the figures, there is at least 60% (calculated by the ratio of peak areas) remaining of the P–O group on Ti substrate surface after 12 days cultivation. These demonstrate the effective coating of bioactive components and lasting on substrate surface during the *in vitro* culture [39].

Moreover, the functionalization of chemical on the substrate surface lead to significant change of feature and also phosphorus element content base on the AFM and XPS results, just as the broadening of the P–O lines (in XPS data), while among them the chemical shift to higher binding energy (0.5eV) in most of the figures after functionalization has been linked to the oxidative doping of Ac-BP molecules. Meanwhile, the unavoidable exposure to oxygen and moisture, as well as the contamination during handling, that might account for the tiny P–O peaks of the bold Ti surface (control) without coating.

3.3. Titanium screws bio-functionalized with N-cadherin mimetic peptide via Ac-BP promoted the osseointegration and bone formation in vivo

After 8 weeks of implantation, the bio-functionalized titanium screws conjugated with the biomimetic peptide via Ac-BP were

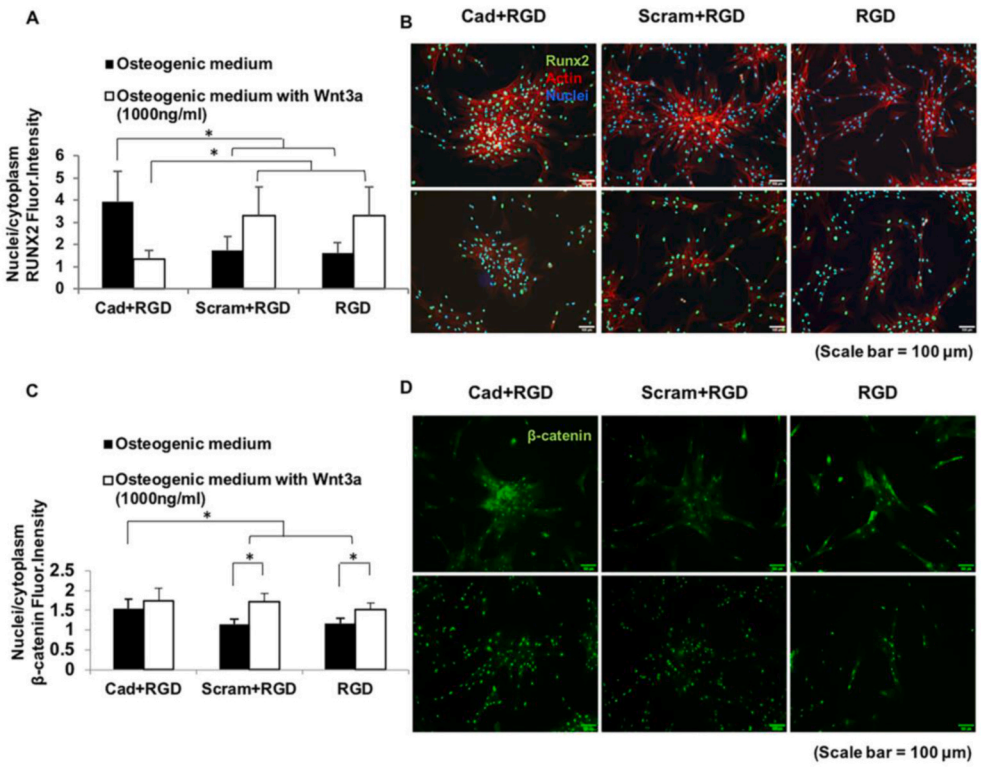

Fig. 6. (A) RUNX2 expression was reduced by Wnt 3a in the Cad + RGD group. (B) RUNX2 immunofluorescent staining in the hBMSCs on biomimetic peptide/Ac-BP conjugated 2D substrate (upper row) and Wnt 3a mimetic peptide supplementation significantly reduced RUNX2 expression (lower row). (n = 60 cells, **p value < 0.01, scale bar = 100 μm). (C) β-catenin immunostaining means fluorescent intensity ratio and (D) corresponding images for hMSCs on N-cadherin/RGD conjugated hydrogels (upper row) and Wnt 3a mimetic peptide supplemented group (lower row) after osteogenesis for 6 days. The quantitative analysis show that the grafted N-cadherin mimetic peptide promoted the β-catenin expression, and supplementation of Wnt 3a mimetic peptide suppressed the β-catenin expression promoted by the conjugated N-cadherin mimetic peptide. (n = 60 cells, *p value < 0.05, scale bar = 100 μm).

harvested for the sample analysis (Fig. 1B). Micro-computed tomography (micro CT) reconstruction revealed substantially more new bone formation in the tibia/femur implanted with N-cadherin mimetic peptide/Ac-BP-conjugated screws (Cad + RGD), when compared to the other control groups (Fig. 3A). Calcein/xylenol double labeling suggested accelerated new-bone formation in the Cad + RGD group from week 6–8, when compared to the other control groups (Fig. 3C) [3].

The effects of conjugated biomimetic peptide and Ac-BP on the parameters of proximal tibiae/femurs metaphysis cancellous bone formation were shown in Fig. 3D [40,41]. The dynamic bone formation parameters (Ir. L. Wi/Ir. L.Th, SL. S/BS) were significantly increased in the Cad + RGD group. There was no significant difference in the static parameters (LS/BS, dL. S/BS) among all the groups.

3.4. Implant histological examinations revealed enhanced bone deposition on the N-cadherin peptide-functionalized screw surface

After eight weeks of implantation, rabbit tibiae/femurs with the implanted screws were harvested for analysis. 200 μm undecalcified MMA sections with the implants were stained by Methyl Blue (Fig. 4A), while the samples after the analysis of the torque removal force were decalcified, embedded in paraffin and sectioned (5 μm) for Hematoxylin and Eosin (H&E) staining and the immunohistochemistry analysis (Fig. 4B). In the untreated control group (Control), there was a clear and thin gap between the TiO_2 screws surface and the tibiae/femurs bone tissues (Fig. 4A). Nevertheless, in the groups of screws conjugated with N-cadherin/RGD mimetic peptide and Ac-BP, the bony tissue formed and were in direct contact with the screw surfaces as evidenced by visible Methyl Blue staining (Fig. 4A). There was more bony tissue was seen in the N-cadherin mimetic peptide-conjugated group (Cad + RGD) when compared to the control groups (Scram + RGD, RGD and control) (Fig. 4A).

Enhancements of tissue repair and implant integration are the ultimate goal for metal implant surface modification. Herein, we examined the effect of biomimetic peptide together with Ac-BP on implant osseointegration ability [42,43]. The removal torque forces for different surface modification groups were shown in Fig. 3B. The implant screws conjugated with the N-cadherin mimetic peptide via Ac-BP molecules have significantly higher removal torque force compared to other control screws (Scram + RGD and RGD).

The hematoxylin/eosin staining on the histological sections of paraffin embedded tibiae/femurs samples showed more bone matrix in the Cad + RGD group than those in the Scram + RGD group and the other control groups (RGD and Control) (Fig. 4B). In particular, there were distinct gaps between the bony tissues and screws (Fig. 4B), which was consistent with the methyl blue staining results (Fig. 4A). The immunostaining data showed more intense staining of the RUNX2, SOX9 and Osteocalcin in the N-cadherin mimetic peptide-conjugated group, and this demonstrated that the osseointegration was significantly enhanced in the group conjugated with N-cadherin biomimetic peptide.

3.5. N-cadherin biomimetic peptide promoted osteogenesis and bone formation through Wnt/β-catenin in vitro

To explore the potentially involved signaling pathways, the gene expression and the specific protein markers were investigated in the hMSCs cultured on the surface of the peptide-conjugated titanium substrates. Compared to the control groups (Scram + RGD, RGD), the titanium substrates conjugated with N-cadherin/RGD mimetic peptide and Ac-BP significantly upregulated the mRNA expression of Wnt/β-catenin signaling pathway (Fig. 5A), including N-cadherin (29.7% higher vs. Scram + RGD, 43.8% higher vs. RGD), β-catenin (33.7% higher vs. Scram + RGD), TCF (30.4% higher vs. RGD) and GSK 3β (44.2% lower vs. Scram + RGD, 32.0% lower vs. RGD), at day 4 following the osteogenic differentiation (Fig. 5C). Gene expression of the PI3K/AKT axis (Fig. 5B) showed that PI3K (21.1% higher vs. RGD) and PTEN (59.6% higher vs. Scram + RGD, 42.49% higher vs. RGD) were significantly upregulated during the osteogenesis process at day 4, whereas no significant difference in AKT1 expression was seen (Fig. 5D). Wnt/β-catenin and the PI3K/AKT expression at day 12 following osteogenic differentiation in the hMSCs were also examined (Fig. S4). β-catenin expression at both mRNA and protein levels was significantly

upregulated in the N-cadherin mimetic peptide/Ac-BP group (Cad + RGD) (Fig. 5C, E). N-cadherin mimetic peptide/Ac-BP activated the luciferase activity of β-catenin, indicating that the peptide surface coating activated the Wnt/β-catenin signaling pathway during hMSCs osteogenic differentiation (Fig. 5F).

3.6. Addition of free Wnt 3a mimetic peptide in media inhibited the osteogenesis of hMSCs by downregulating the Wnt/β-catenin signaling pathway

Human MSCs seeded on the 2D biomimetic peptide/Ac-BP-functionalized titanium substrates were stained with the RUNX2 and β-catenin, more intense (128% increase vs. Scram + RGD, 147% increase vs. RGD) RUNX2 staining was seen in the N-cadherin mimetic peptide/Ac-BP conjugated group (Cad + RGD), when compared to the other control groups (Scram + RGD and RGD) (Fig. 6A and B). While the supplementation of free Wnt 3a mimetic peptide inhibited the upregulation of RUNX2 expression (59.8% decrease vs. Scram + RGD, 59.8% decrease vs. RGD (Fig. 6A and B)). The similar trend was also found for the β-catenin immunofluorescence staining; the N-cadherin mimetic peptide promoted the β-catenin expression (33.9% increase vs. Scram + RGD, 32.8% increase vs. RGD), and supplementation of Wnt 3a mimetic peptide suppressed the β-catenin expression promoted by the conjugated N-cadherin mimetic peptide.

The osteogenic markers (Osterix and Osteomodulin) were significantly upregulated at day 4 in the N-cadherin mimetic peptide/Ac-BP group (no significant difference was found at day 12) (Fig. 2A). Significantly more RUNX2 immunostaining was seen in the hMSCs seeded on the N-cadherin mimetic peptide conjugated titanium surface group compared to other control groups (Fig. 2B). These results indicated that the peptide conjugation promoted early osteogenic differentiation of hMSCs. The RUNX2 and β-catenin immunofluorescent staining showed that hMSCs formed cell clusters after six days of *in vitro* osteogenesis (Fig. 6). The cluster size and the percentage of positive immunofluorescent staining areas of both RUNX2 and β-catenin increased in the N-cadherin mimetic peptide conjugated group. This was consistent with our previous published results [3], that the mesenchymal condensation during the osteogenic differentiation was enhanced.

4. Discussion

N-cadherin is a transmembrane protein, which has been considered to be the key factor in directing cell-cell interaction during the mesenchymal condensation. While, the mesenchymal aggregates, formed by the cell-cell interaction, is the earliest morphogenic events preceding some musculoskeletal tissue including cartilage and bone [1,2]. The results and previous data [3] elucidate that the conjugation of N-cadherin mimetic peptide would enhance the osteogenic differentiation of the seeded hMSCs, thereby leading to more bone matrix deposition on the titanium substrates and implants.

Titanium implants, own the merits as high mechanical strength, corrosion resistance, and excellent biocompatibility, have been widely applied to the orthopedic and dental implants [44]. While, the bioinert properties, as the poor bone cell adhesion behavior [7,45], the poor corrosion and abrasion resistance impose restrictions on the biomedical application of titanium implants as well [13]. According to the immunofluorescent images (Fig. 2B), titanium substrate support MSCs adhesion during the *in vitro* culture. However, studies show the insertion of metal implants in bone would damage the bone matrix and cause the disruption of the microcirculation in area [46,47]. In our study, we would like to find out the synergistic effect of the N-cadherin mimetic peptide conjugated with Ti on the promotion of seeded MSCs osteogenesis, and the osseointegration of Ti implants.

As reported, bisphosphonates on one hand suppress osteoclastic activity, on the other hand inhibit resorption of bone matrix [27,28]. In our study, we use the acryloyl-bisphosphonate (Ac-BP) as the linker molecule connecting the N-cadherin mimetic peptide and the titanium substrates (or Ti implants). The biomimetic peptides are conjugated with the Acryloyl-bisphosphonate (Ac-BP) molecule by the reaction between the thiol group of the C-terminal of peptide and the double bond of the molecule of acryloyl group. As we known, the RGD mimetic peptide would directing the cell adhesion on biomaterials [48]. In our previous study [3], data also demonstrated RGD mimetic peptide promote the hMSCs adhesion on the HA hydrogel scaffold,[1] but won't promote cell osteogenesis (even coupled with the scrambled N-cadherin mimetic peptide) at the same coupling conditions when compared with control group.[2] By the result of immunofluorescent images in this study (Fig. 2B), there are no significant differences of MSCs adhesion and osteogenic marker (RUNX2) expression between the RGD[3] conjugated Ti substrate group (RGD[4]) and bold Ti substrate group (Control), which demonstrates the grafting of Ac-BP linker molecule would not influence the ratio of MSCs adhesion and osteogenesis during the *in vitro* differentiation culture. Moreover, the decoupled effect of RGD ligation result in altered interpretation of ECM, by changing the YAP/TAZ localization has been studied by researchers [5,49]. In the future, we may dedicate more work to learn about the relationship between the mechanical property of extracellular microenvironment and the cell-cell interactions mediated by N-cadherin.

The Acryloyl-bisphosphonate (Ac-BP) is adopted as linker molecule, other than the methacrylated hyaluronic acid-bisphosphonate (MeHA-BP) or the MeHA-catechol, which won't cause the nonspecific adsorption or bridging effect by introducing gel structure. Furthermore, the methacrylated groups of the hyaluronic molecule (MeHA-BP/MeHA-catechol) may form gelation structure during the 37 °C and pH 8.0 reacting condition, and this would change the moduli of substrate surface, which may gain significant influence on the osteogenic lineage of seeded MSCs by changing corresponding cellular behavior of mechanotransduction [50]. Results by other studies enhanced the understanding of the bone differentiation processes and determined the optimal stiffness to promote osteogenesis [51]. In our study, the earlier observation of MSCs osteogenesis by increased early marker (RUNX2) expression after four days of *in vitro* osteogenesis, when compared with the 6 days immunofluorescent staining images of MSCs on 2D hydrogel substrates in our previous work [3]. This difference should mainly owe to the increased moduli of metal substrate to the hydrogel scaffold (10–20 kpa of hyaluronic acid hydrogel). MeHA-BP/MeHA-catechol is the chemical which is commonly used for bioactive molecule conjugation on metal substrate. This part of study should gain more attention in our future study, to learn the influence of seeded cell behavior when the biomimetic peptide is conjugated on the metal surface with MeHA-BP or MeHA-catechol molecule.

In each of the experimental groups in the study (except the Control group), the same mole ratio of RGD mimetic (the same mole ratio to the N-cadherin/Scrambled N-cadherin mimetic peptide) were conjugated on the titanium surface (Fig. 2). Although, the RGD mimetic peptide, as one of the components of fibronectin, is reported to improve cell adhesion on biomaterial scaffolds [3,45]. The titanium substrates support MSCs adhesion. While, the ratio of MSCs on the substrate surface between the experimental groups (Cad + RGD, Scram + RGD and RGD) and the Control group (Control) have no significant difference, especially between the RGD mimetic peptide conjugated group (RGD) and the Control group (Control). This elucidate that, the conjugation of biomimetic peptide won't significantly change the MSCs adhesion behavior, the increased cell adhesion ratio of the experimental group (Cad + RGD) should attribute to the increased cell-cell interaction mediated by the N-cadherin mimetic peptide as reported in our previous

[1] Ref. 3: N6.
[2] Ref. 3: Fig. 5.
[3] Biomimetic peptide RGD: adhesive motif from fibronectin.
[4] Group (RGD): please refer to the part of Abbreviation.

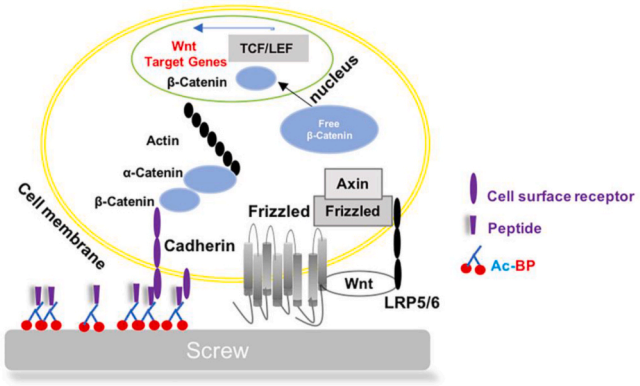

Fig. 7. Schematic diagram showing the possible mechanisms of Wnt/β-catenin axis in osteogenic differentiation and bone formation. Cadherins, including N-cadherins, interact with actin structures via adaptor proteins, such as α-catenin, and they are involved in mechanotransduction via actomyosin contraction [55–57]. The conjugation of the N-cadherin peptide to the metal surface promotes cell–cell clustering and the osteogenic differentiation of the attached hMSCs. Since that the binding between the native membranous N-cadherin of the hMSC and the N-cadherin peptide conjugated on the HA hydrogels likely better mimics the mechanosensing of the homotypic interaction of the native N-cadherins, and that it is capable of initiating the downstream signaling events required for hMSCs lineage specification.

study [3].

Furthermore, based on the immunofluorescent images of the *in vitro* culture study (Fig. 2B) and the *in vivo* study (Figs. 3 and 4), increased expression of early osteogenic marker (RUNX2) and more bone deposition are observed. However, the conjugated Scrambled N-cadherin mimetic peptide (Scram + RGD), when compared with the pure RGD mimetic peptide conjugated group (RGD), neither increased the MSCs adhesion ratio nor the RUNX2 expression. These demonstrate the specific role of N-cadherin mimetic peptide that mediating the increased osteogenesis of MSCs and osseointegration of in situ implant, when coupled with RGD mimetic peptide and Ac-BP molecules.

Base on the images of AFM analysis (Fig. 2C), the grafting of biomimetic peptides and Ac-BP molecule would significantly change the surface topology of titanium substrates, when compared with the titanium substrate group (Control). Previous study has drawn the conclusion, that the osteogenesis of MSCs and the cellular mineralization was significantly stimulated by nanofibrous topology and other factor in a synergistic manner, which was confirmed by the expressions of bone associated genes and proteins [52]. While, in our study, the increased roughness won't change the ratio of cellular adhesion, and the osteogenic marker expression of the seeded MSCs on the 2D substrates (Fig. 2). These may also illustrate the proof of the promoted cell adhesion, MSCs osteogenesis and the increased mineralization are mediated by the N-cadherin mimetic peptide with titanium substrates. Furthermore, more work in future can be done to learn the possible of the synergistic osteogenic promotion by the N-cadherin mimetic peptide and the topology effect of the substrates.

Moreover, as reported in the previous study, Wnt 3a suppress the osteogenic differentiation of MSCs through blocking canonical Wnt signaling (Fig. 7) [53,54]. Studies reported that MSCs osteogenic differentiation was partially inhibited at 100 ng/ml Wnt 3a, whereas 25 ng/ml or lower Wnt 3a failed to inhibit either AP activity or mineralization [54]. In our current study, Wnt 3a mimetic peptide (1000 ng/ml) suppressed the osteogenic differentiation of hMSCs even on the N-cadherin mimetic peptide coated surface (Fig. 6). This finding further confirms that the pro-osteogenic effect of N-cadherin mimetic peptide is mediated via the Wnt/β-catenin signaling.

5. Conclusion

In this study, we demonstrated the synergistic effect of N-cadherin mimetic peptide when coupled with the titanium substrates and implants to promote the osteogenic differentiation of seeded hMSCs and osseointegration of the treated implants. The finding highlights the promotion effect of bioactive molecules to the metal implants. And the cellular and animal models in the current study may serve as a platform for the studies of surface biofunctionalization.

Author contributions

M.L.Z. had collected all of the data in the study and take responsibility for the integrity of the data and the accuracy of the data analysis.

Study design, analysis conception and design. G.L., L.M.B., M.L.Z. and K.Y.Z.

Execution, analysis and interpretation of data. M.L.Z., K.Y.Z., L.F., S. E.L., Q.P.

Drafting and revising the article. M.L.Z., G.L., L.M.B.

All authors approved the final version of the manuscript.

Declaration of competing interest

The authors confirm that there are no conflicts of interest associated with this publication.

Acknowledgements

The work was partially supported by grants from Hong Kong Government Research Grant Council, General Research Fund (14120118, 14160917, 14120118, 14108720 and T13-402/17-N); National Natural Science Foundation of China (81772322); Health and Medical Research Fund, Hong Kong (16170951 and 17180831); Hong Kong Innovation Technology Commission Funds (PRP/050/19FX). This study was also supported in part by SMART program, Lui Che Woo Institute of Innovative Medicine, The Chinese University of Hong Kong and the research was made possible by resources donated by Lui Che Woo Foundation Limited.

Abbreviation

Cad	N-cadherin mimetic peptide
Scram	Scrambled sequence N-cadherin mimetic peptide
RGD	Ac-BP: Acryloyl bisphosphonate
Ti	Titanium substrates/screws
Group (Cad + RGD)	Cad + RGD + Ac-BP + Ti
Group (Scram + RGD)	Scram + RGD + Ac-BP + Ti
Group (RGD)	RGD + Ac-BP + Ti
Group (Control)	Ti
TCEP	tris (2-carboxyethyl) phosphine
PVDF membrane	Polyvinylidene fluoride membrane
DXA	DXA (Dual-energy x-ray absorptiometry) analysis
MMA	methyl methacrylate

Appendix A. Supplementary data

Supplementary data to this article can be found online at https://doi.org/10.1016/j.bioactmat.2020.11.002.

References

[1] A.M. DeLise, R.S. Tuan, Alterations in the spatiotemporal expression pattern and function of N-cadherin inhibit cellular condensation and chondrogenesis of limb mesenchymal cells in vitro, J. Cell. Biochem. 87 (3) (2002) 342–359.

[2] S.A. Oberlender, R.S. Tuan, Spatiotemporal profile of N-cadherin expression in the developing limb mesenchyme, Cell Adhes. Commun. 2 (6) (1994) 521–537.

[3] M.L. Zhu, S. Lin, Y.X. Sun, Q. Feng, G. Li, L.M. Bian, Hydrogels functionalized with N-cadherin mimetic peptide enhance osteogenesis of hMSCs by emulating the osteogenic niche, Biomaterials 77 (2016) 44–52.
[4] L.M. Bian, M. Guvendiren, R.L. Mauck, J.A. Burdick, Hydrogels that mimic developmentally relevant matrix and N-cadherin interactions enhance MSC chondrogenesis, Proc. Natl. Acad. Sci. U. S. A. 110 (25) (2013) 10117–10122.
[5] B.D. Cosgrove, K.L. Mui, T.P. Driscoll, S.R. Caliari, K.D. Mehta, R.K. Assoian, J. A. Burdick, R.L. Mauck, N-cadherin adhesive interactions modulate matrix mechanosensing and fate commitment of mesenchymal stem cells, Nat. Mater. 15 (12) (2016) 1297–1306.
[6] H. Yazici, H. Fong, B. Wilson, E.E. Oren, F.A. Amos, H. Zhang, J.S. Evans, M. L. Snead, M. Sarikaya, C. Tamerler, Biological response on a titanium implant-grade surface functionalized with modular peptides, Acta Biomater. 9 (2) (2013) 5341–5352.
[7] M. Pagel, R. Hassert, T. John, K. Braun, M. Wiessler, B. Abel, A.G. Beck-Sickinger, Multifunctional coating improves cell adhesion on titanium by using cooperatively acting peptides, Angew. Chem. Int. Ed. 55 (15) (2016) 4826–4830.
[8] D. Schwartz-Arad, A. Laviv, L. Levin, Failure causes, timing, and cluster behavior: an 8-year study of dental implants, Implant Dent. 17 (2) (2008) 200–207.
[9] S.L. Wu, Z.Y. Weng, X.M. Liu, K.W.K. Yeung, P.K. Chu, Functionalized TiO2 based nanomaterials for biomedical applications, Adv. Funct. Mater. 24 (35) (2014) 5464–5481.
[10] M. He, X.Y. Chen, K. Cheng, W.J. Weng, H.M. Wang, Enhanced osteogenic activity of TiO2 nanorod films with microscaled distribution of Zn-CaP, ACS Appl. Mater. Interfaces 8 (11) (2016) 6944–6952.
[11] R.I.M. Asri, W.S.W. Harun, M. Samykano, N.A.C. Lah, S.A.C. Ghani, F. Tarlochan, M.R. Raza, Corrosion and surface modification on biocompatible metals: a review, Mater. Sci. Eng. C Mater. Biol. Appl. 77 (2017) 1261–1274.
[12] M. Ting, S.R. Jefferies, W. Xia, H. Engqvist, J.B. Suzuki, Classification and effects of implant surface modification on the bone: human cell-based in vitro studies, J. Oral Implantol. 43 (1) (2017) 58–83.
[13] J.S. Lee, K. Kim, J.P. Park, S.W. Cho, H. Lee, Role of pyridoxal 5 '-Phosphate at the titanium implant interface in vivo: increased hemophilicity, inactive platelet adhesion, and osteointegration, Adv. Healthc. Mater. 6 (5) (2017).
[14] Y.C. Shi, L.T. Wang, Y.M. Niu, N. Yu, P.F. Xing, L. Dong, C.M. Wang, Fungal component coating enhances titanium implant-bone integration, Adv. Funct. Mater. 28 (46) (2018).
[15] K. Das, S. Bose, A. Bandyopadhyay, Surface modifications and cell-materials interactions with anodized Ti, Acta Biomater. 3 (4) (2007) 573–585.
[16] S. VandeVondele, J. Voros, J.A. Hubbell, RGD-Grafted poly-l-lysine-graft-(polyethylene glycol) copolymers block non-specific protein adsorption while promoting cell adhesion, Biotechnol. Bioeng. 82 (7) (2003) 784–790.
[17] W. Tang, G.M. Policastro, G. Hua, K. Guo, J.J. Zhou, C. Wesdemiotis, G.L. Doll, M. L. Becker, Bioactive surface modification of metal oxides via catechol-bearing modular peptides: multivalent-binding, surface retention, and peptide bioactivity, J. Am. Chem. Soc. 136 (46) (2014) 16357–16367.
[18] G. Balasundaram, C. Yao, T.J. Webster, TiO2 nanotubes functionalized with regions of bone morphogenetic protein-2 increases osteoblast adhesion, J. Biomed. Mater. Res. 84a (2) (2008) 447–453.
[19] I. Wall, N. Donos, K. Carlqvist, F. Jones, P. Brett, Modified titanium surfaces promote accelerated osteogenic differentiation of mesenchymal stromal cells in vitro, Bone 45 (1) (2009) 17–26.
[20] A. Bagno, A. Piovan, M. Dettin, A. Chiarion, P. Brun, R. Gambaretto, G. Fontana, C. Di Bello, G. Palu, I. Castagliuolo, Human osteoblast-like cell adhesion on titanium substrates covalently functionalized with synthetic peptides, Bone 40 (3) (2007) 693–699.
[21] Y.J. Seol, Y.J. Park, S.C. Lee, K.H. Kim, J.Y. Lee, T.I. Kim, Y.M. Lee, Y. Ku, I. C. Rhyu, S.B. Han, C.P. Chung, Enhanced osteogenic promotion around dental implants with synthetic binding motif mimicking bone morphogenetic protein (BMP)-2, J. Biomed. Mater. Res. 77a (3) (2006) 599–607.
[22] K.Y. Zhang, Q. Feng, J.B. Xu, X.Y. Xu, F. Tian, K.W.K. Yeung, L.M. Bian, Self-assembled injectable nanocomposite hydrogels stabilized by bisphosphonate-magnesium (Mg2+) coordination regulates the differentiation of encapsulated stem cells via dual crosslinking, Adv. Funct. Mater. 27 (34) (2017).
[23] E.V. Giger, B. Castagner, J. Raikkonen, J. Monkkonen, J.C. Leroux, siRNA transfection with calcium phosphate nanoparticles stabilized with PEGylated chelators, Adv. Healthc. Mater. 2 (1) (2013) 134–144.
[24] T. Sato, M. Ebara, S. Tanaka, T.A. Asoh, A. Kikuchi, T. Aoyagi, Rapid self-healable poly(ethylene glycol) hydrogels formed by selective metal-phosphate interactions, Phys. Chem. Chem. Phys. 15 (26) (2013) 10628–10635.
[25] L.E. Cole, T. Vargo-Gogola, R.K. Roeder, Targeted delivery to bone and mineral deposits using bisphosphonate ligands, Adv. Drug Deliv. Rev. 99 (2016) 12–27.
[26] H. Kajiwara, T. Yamaza, M. Yoshinari, T. Goto, S. Iyama, I. Atsuta, M.A. Kido, T. Tanaka, The bisphosphonate pamidronate on the surface of titanium stimulates bone formation around tibial implants in rats, Biomaterials 26 (6) (2005) 581–587.
[27] P. Duan, L.F. Bonewald, The role of the wnt/beta-catenin signaling pathway in formation and maintenance of bone and teeth, Int. J. Biochem. Cell Biol. 77 (Pt A) (2016) 23–29.
[28] K.F. Wu, W.C. Liang, L. Feng, J.X. Pang, M.M. Waye, J.F. Zhang, W.M. Fu, H19 mediates methotrexate resistance in colorectal cancer through activating Wnt/beta-catenin pathway, Exp. Cell Res. 350 (2) (2017) 312–317.
[29] S.L. Ferrari, K. Traianedes, M. Thorne, M.H. Lafage-Proust, P. Genever, M. G. Cecchini, V. Behar, A. Bisello, M. Chorev, M. Rosenblatt, L.J. Suva, A role for N-cadherin in the development of the differentiated osteoblastic phenotype, J. Bone Miner. Res. 15 (2) (2000) 198–208.
[30] P.J. Marie, E. Hay, Cadherins and Wnt signalling: a functional link controlling bone formation, BoneKEy Rep. 2 (2013) 330.
[31] A. Di Benedetto, M. Watkins, S. Grimston, V. Salazar, C. Donsante, G. Mbalaviele, G.L. Radice, R. Civitelli, N-cadherin and cadherin 11 modulate postnatal bone growth and osteoblast differentiation by distinct mechanisms, J. Cell Sci. 123 (15) (2010) 2640–2648.
[32] P.J. Marie, Role of N-cadherin in bone formation, J. Cell. Physiol. 190 (3) (2002) 297–305.
[33] A.R. Guntur, C.J. Rosen, M.C. Naski, N-cadherin adherens junctions mediate osteogenesis through PI3K signaling, Bone 50 (1) (2012) 54–62.
[34] E. Hay, A. Nouraud, P.J. Marie, N-cadherin negatively regulates osteoblast proliferation and survival by antagonizing wnt, ERK and PI3K/akt signalling, PloS One 4 (12) (2009).
[35] L. Wang, M. Zhang, Z. Yang, B. Xu, The first pamidronate containing polymer and copolymer, Chem. Commun. (26) (2006) 2795–2797.
[36] Y.F. Zhang, J.K. Xu, Y.C. Ruan, M.K. Yu, M. O'Laughlin, H. Wise, D. Chen, L. Tian, D.F. Shi, J.L. Wang, S.H. Chen, J.Q. Feng, D.H.K. Chow, X.H. Xie, L.Z. Zheng, L. Huang, S. Huang, K. Leung, N. Lu, L. Zhao, H.F. Li, D.W. Zhao, X. Guo, K. M. Chan, F. Witte, H.C. Chan, Y.F. Zheng, L. Qin, Implant-derived magnesium induces local neuronal production of CGRP to improve bone-fracture healing in rats, Nat. Med. 22 (10) (2016) 1160–1169.
[37] G. Zhang, B.S. Guo, H. Wu, T. Tang, B.T. Zhang, L.Z. Zheng, Y.X. He, Z.J. Yang, X. H. Pan, H. Chow, K. To, Y.P. Li, D.H. Li, X.L. Wang, Y.X. Wang, K. Lee, Z.B. Hou, N. Dong, G. Li, K. Leung, L. Hung, F.C. He, L.Q. Zhang, L. Qin, A delivery system targeting bone formation surfaces to facilitate RNAi-based anabolic therapy, Nat. Med. 18 (2) (2012) 307–314.
[38] P.K. Suen, Y.X. He, D.H.K. Chow, L. Huang, C.Y. Li, H.Z. Ke, M.S. Ominsky, L. Qin, Sclerostin monoclonal antibody enhanced bone fracture healing in an open osteotomy model in rats, J. Orthop. Res. 32 (8) (2014) 997–1005.
[39] J. Wang, Y. Wei, N. Li, J. Chen, Hydration resistance of CaO material prepared by Ca(OH)2 calcination with chelating compound, Materials 12 (14) (2019).
[40] D.W. Dempster, J.E. Compston, M.K. Drezner, F.H. Glorieux, J.A. Kanis, H. Malluche, P.J. Meunier, S.M. Ott, R.R. Recker, A.M. Parfitt, Standardized nomenclature, symbols, and units for bone histomorphometry: a 2012 update of the report of the ASBMR Histomorphometry Nomenclature Committee, J. Bone Miner. Res. 28 (1) (2013) 2–17.
[41] S. Lin, J. Huang, L. Zheng, Y. Liu, G. Liu, N. Li, K. Wang, L. Zou, T. Wu, L. Qin, L. Cui, G. Li, Glucocorticoid-induced osteoporosis in growing rats, Calcif. Tissue Int. 95 (4) (2014) 362–373.
[42] L.W. Lin, H. Wang, M. Ni, Y.F. Rui, T.Y. Cheng, C.K. Cheng, X.H. Pan, G. Li, C. J. Lin, Enhanced osteointegration of medical titanium implant with surface modifications in micro/nanoscale structures, J. Orthop. Transl. 2 (1) (2014) 35–42.
[43] T.A. Petrie, J.E. Raynor, D.W. Dumbauld, T.T. Lee, S. Jagtap, K.L. Templeman, D. M. Collard, A.J. Garcia, Multivalent integrin-specific ligands enhance tissue healing and biomaterial integration, Sci. Transl. Med. 2 (45) (2010).
[44] C.Y. Chien, W.B. Tsai, Poly(dopamine)-assisted immobilization of Arg-Gly-Asp peptides, hydroxyapatite, and bone morphogenic protein-2 on titanium to improve the osteogenesis of bone marrow stem cells, ACS Appl. Mater. Interfaces 5 (15) (2013) 6975–6983.
[45] G. Vidal, T. Blanchi, A.J. Mieszawska, R. Calabrese, C. Rossi, P. Vigneron, J. L. Duval, D.L. Kaplan, C. Egles, Enhanced cellular adhesion on titanium by silk functionalized with titanium binding and RGD peptides, Acta Biomater. 9 (1) (2013) 4935–4943.
[46] P. Tengvall, B. Skoglund, A. Askendal, P. Aspenberg, Surface immobilized bisphosphonate improves stainless-steel screw fixation in rats, Biomaterials 25 (11) (2004) 2133–2138.
[47] L. Cardoso, B.C. Herman, O. Verborgt, D. Laudier, R.J. Majeska, M.B. Schaffler, Osteocyte apoptosis controls activation of intracortical resorption in response to bone fatigue, J. Bone Miner. Res. 24 (4) (2009) 597–605.
[48] S.L. Bellis, Advantages of RGD peptides for directing cell association with biomaterials, Biomaterials 32 (18) (2011) 4205–4210.
[49] R. Li, S. Lin, M. Zhu, Y. Deng, X. Chen, K. Wei, J. Xu, G. Li, L. Bian, Synthetic presentation of noncanonical Wnt5a motif promotes mechanosensing-dependent differentiation of stem cells and regeneration, Sci. Adv. 5 (10) (2019), eaaw3896.
[50] A. Tajik, Y. Zhang, F. Wei, J. Sun, Q. Jia, W. Zhou, R. Singh, N. Khanna, A. S. Belmont, N. Wang, Transcription upregulation via force-induced direct stretching of chromatin, Nat. Mater. 15 (12) (2016) 1287–1296.
[51] C. Luo, H. Fang, M. Zhou, J. Li, X. Zhang, S. Liu, C. Zhou, J. Hou, H. He, J. Sun, Z. Wang, Biomimetic open porous structured core-shell microtissue with enhanced mechanical properties for bottom-up bone tissue engineering, Theranostics 9 (16) (2019) 4663–4677.
[52] J.J. Kim, A. El-Fiqi, H.W. Kim, Synergetic cues of bioactive nanoparticles and nanofibrous structure in bone scaffolds to stimulate osteogenesis and angiogenesis, ACS Appl. Mater. Interfaces 9 (3) (2017) 2059–2073.
[53] G.M. Boland, G. Perkins, D.J. Hall, R.S. Tuan, Wnt 3a promotes proliferation and suppresses osteogenic differentiation of adult human mesenchymal stem cells, J. Cell. Biochem. 93 (6) (2004) 1210–1230.
[54] G.Z. Liu, S. Vijayakumar, L. Grumolato, R. Arroyave, H.F. Qiao, G. Akiri, S. A. Aaronson, Canonical Wnts function as potent regulators of osteogenesis by human mesenchymal stem cells, J. Cell Biol. 185 (1) (2009) 67–75.

[55] D.E. Leckband, Q. le Duc, N. Wang, J. de Rooij, Mechanotransduction at cadherin-mediated adhesions, Curr. Opin. Cell Biol. 23 (5) (2011) 523–530.
[56] B. Ladoux, E. Anon, M. Lambert, A. Rabodzey, P. Hersen, A. Buguin, P. Silberzan, R.M. Mege, Strength dependence of cadherin-mediated adhesions, Biophys. J. 98 (4) (2010) 534–542.
[57] S. Yonemura, Y. Wada, T. Watanabe, A. Nagafuchi, M. Shibata, alpha-Catenin as a tension transducer that induces adherens junction development, Nat. Cell Biol. 12 (6) (2010) 533–542.